Tailoring the Effective Properties of *Typha* Fiber Reinforced Polymer Composite via Alkali Treatment

Samsul Rizal,[a] Ikramullah,[a] Deepu A. Gopakumar,[b] Syifaul Huzni,[a] Sulaiman Thalib,[a] M. I. Syakir,[b] F. A. T. Owolabi,[b,c] N. A. Sri Aprilla,[d] M. T. Paridah,[e]* and H. P. S. Abdul Khalil [b,]*

Typha fibers were chemically retted in 5% sodium hydroxide solution for 1 h, 2 h, 4 h, and 8 h. Changes in chemical compositions of the untreated and treated fibers were monitored with Fourier transmission infrared spectroscopy, while changes in the crystallinity index were studied *via* X-ray diffraction. The FTIR spectra and scanning electron microscope images corroborated the successful removal of amorphous portions from the *Typha* leaf fibers during alkali treatment, which resulted in an enhanced crystallinity index for alkali-treated fibers. The alkali-treated *Typha* fiber for 1 h showed the highest water contact angle of 87.5°, while the untreated composite showed the lowest contact angle. Typha fiber treated for 4 h had high tensile strength, Young's modulus, and elongation at break of 158 MPa, 1600 MPa, and 7%, respectively. The results showed that there was a general increase in the interfacial shear strength of *Typha* fiber with epoxy resin and polyester resin with increased time. Both the mechanical properties and crystallinity index of the *Typha* leaf fibers increased with increased time of retting until 4 h, after which further alkaline retting resulted in decreased values. The overall results showed that alkaline-extracted *Typha* leaf fibers are suitable for biodegradable film composites.

Keywords: *Typha fiber characterization; Mechanical performance; Interfacial shear strength; Microbond test*

Contact information: a: Department of Mechanical Engineering, Universitas Syiah Kuala, Banda Aceh 23111, Indonesia; b: School of Industrial Technology, Universiti Sains Malaysia, 11800 Penang, Malaysia; c: Pulp and Paper Technology Laboratory, Federal Institute of Industrial Research Oshodi, Lagos, Nigeria; d: Department of Chemical Engineering, Universitas Syiah Kuala, Banda Aceh 23111, Indonesia; e: Institutes of Tropical Forestry and Forest Products (INTROP), Universiti Putra Malaysia, 43400 Serdang, Selangor, Malaysia;
** Corresponding author: parida.introp@gmail.com; akhalilhps@gmail.com*

INTRODUCTION

Natural fibers have gained considerable interest for researchers, engineers, and scientists as an alternative reinforcement for fiber-reinforced polymer (FRP) composites due to their low cost, fairly good mechanical properties, non-abrasive character, eco-friendliness, and bio-degradability. They could be exploited as a replacement for various conventional fiber types, such as glass, aramid, and carbon. A wide range of natural fibers such as wood fibers, stem fibers, and leaf fibers have been used to strengthen polymer composites (Jawaid and Abdul Khalil 2011). Among the natural fibers, *Typha* fibers have received great attention due to their abundant nature. *Typha* fiber is widely available in most countries and is wildly grown on wetlands in the province of Aceh, Indonesia (Majeed *et al*. 2013). Although *Typha* is abundantly available in nature, its potential is still

underutilized compared to other natural fibers. In recent decades, natural fiber-reinforced polymer composites have begun to compete with synthetic fiber-reinforced composites, such as glass fibers and carbon fibers, because they have many advantages over glass fibers and carbon fibers (Jawaid and Abdul Khalil 2011; Majeed *et al.* 2013). Natural fibers may present certain mechanical properties equal or superior to those of glass fibers (Taylor *et al.* 2017). Other advantages of using natural fibers compared to carbon fibers and glass fibers include low density, reduction in energy consumption, no irritability to the skin, renewability, and biodegradability (Fragassa *et al.* 2018; Ilyas *et al.* 2018b,c). Moreover, natural fibers have low cost with low density and high specific properties compared to synthetic fibers (Jawaid and Abdul Khalil 2011).

For the development and utilization of natural fibers as an effective reinforcement in composites, it is very relevant to know the characteristics of the natural fibers. Natural fibers are generally hydrophilic, which makes natural fibers less compatible with most of the hydrophobic polymeric matrices. This incompatibility between the hydrophobic polymer matrices and hydrophilic natural fibers can result in weak adhesion at the interface between polymer matrix and natural fiber (Majeed *et al.* 2013; Ilyas *et al.* 2017; Sanjay *et al.* 2018). This is one of the reasons why natural fibers have not completely replaced conventional synthetic fiber materials in high-load applications. Natural fiber-reinforced composites have been used in the automotive industry (Al-Oqla and Sapuan 2014), but their application generally has been limited to components such as door panels, chair backs, packaging, and other interior panels (Sanjay *et al.* 2016; Sanyang *et al.* 2018). The different kinds of natural fibers such as jute, hemp, kenaf, oil palm, and bamboo reinforced polymer composite have received a lot of attention in different automotive applications, structural components, packing, and construction (Shalwan and Yousif 2013; Sassoni *et al.* 2014). The wide advantages of natural fibers reinforced composites such as high stiffness to weight ratio, lightweight, and biodegradability give them suitability in different application in the building industries (Ramezani Kakroodi *et al.* 2013).

Due to the rapid growth of the natural fiber industry, surface modification of the natural fibers is relevant to study in order to enhance the interfacial compatibility between the polymer matrix and natural fiber (Taylor *et al.* 2017; Fragassa *et al.* 2018; Sanjay *et al.* 2018). The physicochemical properties of natural fiber-reinforced composites rely on the type of fiber, matrix, and matrix-fiber interface. The interface is an in-between zone of fiber-matrix bonds that is present to distribute the stress obtained by the matrix to the fiber (Loh *et al.* 2013; Ahmad *et al.* 2015; Cohen *et al.* 2016). It is of great importance to note that one type of failure mechanism of a composite is when the tensile force delivered to the fiber is higher than the bonding strength of the fiber-matrix, as this will result in debonding and pull-out fibers of the matrix (Karger-Kocsis *et al.* 2015; Zhao *et al.* 2018). Interfacial shear strength is the friction force received by the matrix that can still be channelled to the fiber through the interface bond. If the fiber and matrix interactions are poor, then the tensile strength of the composite would be relatively low.

An alkali treatment of the fiber is one of the least costly and most often-used methods for increasing the strength of the interface bonds with the polymer matrix (Sanjay *et al.* 2018). This method removes the surface impurities on fiber surface that might harm the fiber-matrix bond. Additionally, it also removes the amorphous portions such as pectin, wax, lignin, and hemicellulose from the natural fiber (Torstensen *et al.* 2018). However, prolonged alkali treatment would affect the cellulosic structure of natural fiber, resulting in the decrement of mechanical properties. The surface roughness of fiber plays a key role in better mechanical bonding with the matrix. Mechanical bonding is an important factor

because it is responsible for the composite's interface strength (Da Silva *et al.* 2018). Methods such as single-fiber pull-out test, fiber-bundle pull-out test, and microbond test were used to evaluate the interfacial shear strength (IFSS) of the fibers (Ferreira *et al.* 2018; Xiong *et al.* 2018). In this context, herein we studied the effect of alkali treatment on the mechanical and physical properties of *Typha* fiber. Additionally, we also determined the effect of alkali treatment on the interfacial strength of *Typha* fibers with both epoxy and polyester resin *via* microbond test.

EXPERIMENTAL

Materials

Typha latifolia plants were collected from swamps in the Darussalam local area, (Banda Aceh, Indonesia) and had lengths from 250 cm to 310 cm and diameters from 9 cm to 14 cm; they were manually decorticated, washed, and dried. Sodium hydroxide (NaOH; with > 98% purity) was purchased from local vendors (Penang, Malaysia), in pellets. Acetic acid (Merck Group, Pulheim Germany) was used for the fiber extraction process. A solution of 5% NaOH was used to soak the fiber for 1 h, 2 h, 4 h, and 8 h; then, the fiber was washed thoroughly with the excess alkali, neutralized by the acetic acid, and then thoroughly washed and combed. The epoxy and polyester resin and hardener used were Araldite LY-564 and HY 560 (mixing ratio 100:27 wt%) from Huntsman Advanced Materials, Basel, Switzerland.

Methods

Fabrication of composite

The untreated and alkali treated *Typha* fibers were dried in the sun for 4 h. Then, the fiber was cut to 200 mm length and compacted by placing fibers between two metal plates. Then the fiber was pressed. A rectangular shape of metal plate with 170 mm x 150 mm x 3 mm was employed as a composite mold. *Typha* fibers of different dimensions were spread on polyester and epoxy resin by a hand layup method. After this, the molds were pressed with 200 kg/cm^2 in the compression molding machine.

Fourier transform infrared spectroscopy (FTIR)

The chemical functional groups of untreated and alkali-treated *Typha* fibers were studied using a Nicolet iS10 Fourier Transform Infrared Spectrometer device equipped with an attenuated total reflectance (ATR) microscope recorded within a wavelength range of 500 cm^{-1} to 4000 cm^{-1} (ThermoFisher, Waltham, MA, USA). The Nicolet FTIR spectrometer was used to record the absorption spectra of *Typha* fibers after 1 mg of the fiber powders were pelletized with 100 mg KBr.

X-ray diffraction (XRD)

The X-ray diffractometer was used to observe the crystalline index of the fiber. The wide-angle XRD spectra of the fibers were recorded on a Bruker D8 Advance (Billerica, USA) diffractometer. All samples were scanned in the range of 2θ from 0 ° to 30 °.

Scanning electron microscopy (SEM)

Detailed morphological images of the untreated and alkali-treated *Typha* fibers' surfaces and microdroplets were observed using a Carl Zeiss Leo Supra 50 VP scanning

electron microscope (Carl Zeiss AG, Oberkochen, Germany) that operated with an accelerating voltage of 15 kV. The sample surface was coated with gold using a Polaron SC515 sputter coater (Ladd Research Industries Inc., Williston, VT, USA) prior to observation.

Tensile testing

The mechanical properties of the fibers were evaluated for their tensile strength, ductility, and modulus of *Typha* fiber elasticity. These tests were performed using a tensile testing machine (Inspect micro S500; Hegewald & Peschke, Nossen, Germany) equipped with a load cell of 10 kN, with a crosshead speed of 2 mm/min with according to ASTM D3379-75 standard. The diameters of *Typha* fibers were measured using Olympus Cell B software (Olympus Corporation, Tokyo, Japan). Ten measurements were taken for each fiber in order obtain the average value of tensile strength.

Contact angle studies

The water contact angle of the fiber was determined using a KSV CAM 101 (Biolin Scientific, Gothenburg, Sweden) optical contact angle meter to examine the surface wettability of the fiber. Hypodermic syringes were employed to drop water onto the fiber surface. The contact angle was measured on the side of the water droplet. The image was recorded for 40 s with a speed of one frame every 10 s. Three measurements were obtained for each sample and the average value was calculated.

Microbond test

The microbond test developed by Miller *et al.* (1987) was conducted to determine the IFSS value. Epoxy and polyester resins were dripped onto the surface of *Typha* fiber, which is called a microdroplet, as shown in Fig. 1, to determine the interfacial shear strength (IFSS) of *Typha* fibers in both matrices.

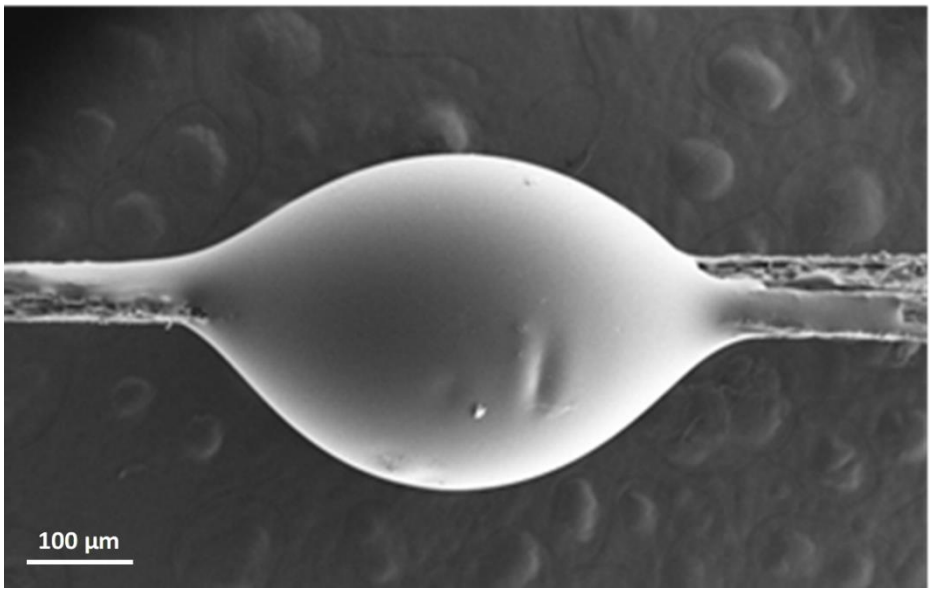

Fig. 1. Microdroplet of polyester resin on the surface of *Typha* fiber

The fibers were withdrawn from the matrix using the tensile test machine. The embedded length of the microdroplet resin was in the range of 1.58 mm to 2.19 mm and the fiber diameters were 0.17 mm to 0.46 mm. The microbond test schematic is presented in Fig. 2. The interfacial shear strength (τ) of the *Typha* fiber was calculated using Eq. 1,

$$\tau = \frac{F_{max}}{\pi D_f L_e} \quad (1)$$

where F_{max} is the maximum load (N), D_f is the fiber diameter (mm), and L_e is the fiber embedded length in the matrix (mm).

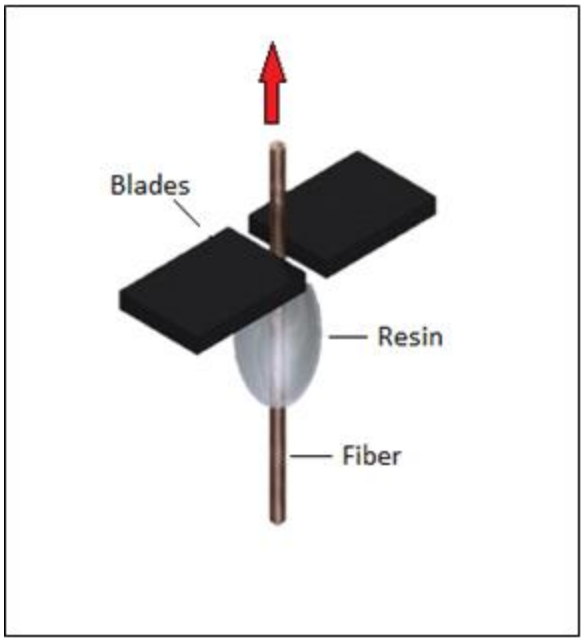

Fig. 2. Schematic of microbond test

RESULTS AND DISCUSSION

FTIR Analysis

The results of the FTIR spectroscopic analysis of the raw and chemically retted *Typha* leaf fibers are presented in Fig. 3. Despite the similarities in the spectra plot, as evidenced by the two main absorbance regions, *i.e.*, the broad region corresponding to the range 3200 cm^{-1} to 3400 cm^{-1} and the functional group region corresponding to 500 cm^{-1} to 1800 cm^{-1}, the various changes observed in the spectra absorption confirmed that there were some changes in the chemical compositions of the treated *Typha* fibers due to the chemical retting process. The FTIR spectra analysis revealed that after the retting process all of the spectra showed a broad band in the region of 3400 cm^{-1} to 3300 cm^{-1}, which indicated the characteristic O-H stretching vibration of the OH group in cellulose fiber molecules (Ilyas *et al.* 2018a), while the spectra band shown in each spectra at around 2900 cm^{-1} was characteristic of C-H stretching vibration (Khalil *et al.* 2001).

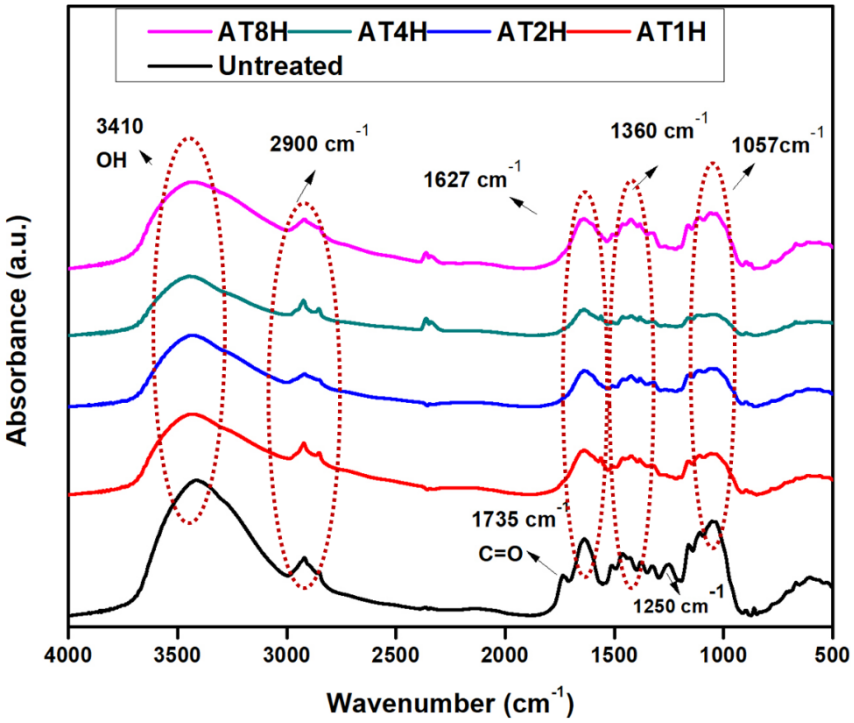

Fig. 3. FTIR spectra of untreated and alkali-treated Typha

Additionally, the vibration peaks detected between 1360 cm^{-1} and 1365 cm^{-1} in both the unretted and chemically retted *Typha* fiber samples were attributable to the bending vibration of the C-O and C–H bonds in the polysaccharide aromatic rings (Nacos *et al.* 2006). The absorbance peak observed around 1057 cm^{-1} was due to the C-O-C pyranose ring skeletal vibration. The spectra results at this peak further showed a gradual increase in the intensity of this band as the treatment time increased, which showed an increase in the crystallinity of the samples (Sun *et al.* 2018). The absorbance band at 1640 cm^{-1} common to all of the spectra was attributable to the OH bending of adsorbed water (Łojewska *et al.* 2005). Despite all of these similarities, specific unique absorbance peaks were identified in the spectra. For instance, the spectral peak at 1735 cm^{-1} for the raw *Typha* was attributed to the C=O stretching vibration of the acetyl and uronic ester groups from pectin, hemicelluloses, or other ester linkages of the carboxylic group of ferulic and p-coumarin acids of lignin or hemicelluloses (Owolabi *et al.* 2017a). The absence of this spectral peak indicated the effective removal of the amorphous portions *via* the alkaline treatment. Lastly, the absorbance peak at 1250 cm^{-1} in the raw fiber spectrum was attributable to the C-O out-of-plane stretching vibration of the aryl group in the lignin (Le Troedec *et al.* 2008). These two peaks completely disappeared in the spectra of the chemically/alkali-treated fibers.

XRD Crystallography of *Typha* Fibers

X-ray diffraction was used to analyze the effect of the cellulose fiber crystallinity on the physical and mechanical properties of the treated fiber. Figure 4 shows an XRD pattern of the raw and the chemically retted *Typha* fibers at different times.

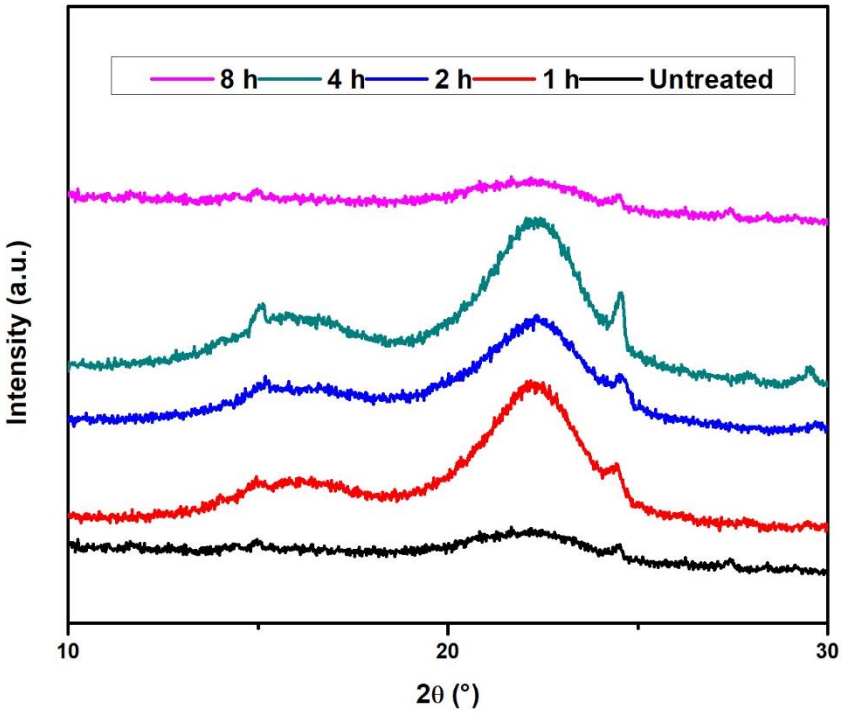

Fig. 4. XRD of treated and untreated *Typha* fiber

All of the diffraction patterns showed peaks around 2θ = 16º, 22.5º, and 24.8º, which indicated the typical cellulose I structure. The only difference in the diffraction pattern was the change in the peak's intensity, which indicated some changes in the fiber crystallinity. The results showed that the peaks at 16º and 22.5º were most defined for the fiber treated at 4 h, and this was attributable to the fact that during chemical retting/alkali treatment the cementing materials, such as tannins, hemicelluloses, and lignin, were dissolved, and the remaining pure crystalline cellulose were isolated. The crystallinity index for both the untreated and treated *Typha* fibers were calculated according to Eq. 2,

$$CI(\%) = \frac{I002 - Iam}{I002} \times 100 \quad (2)$$

The obtained crystallinity index values of the untreated *Typha* fiber and treated *Typha* fibers at 1 h, 2 h, 4 h, and 8 h were 29.6%, 47.5%, 50.3%, 55.8%, and 35.8%, respectively. This trend was expected to correspond to the increasing trend of the mechanical properties of the fibers (Owolabi *et al.* 2017b). The results revealed that the sample with the lowest crystallinity index was the raw *Typha* fiber, and the fiber retted for 4 h had the highest crystallinity index. The increase in crystallinity index was attributed to the removal of amorphous constituents, including hemicellulose, lignin, and pectin, from the *Typha* fiber during the alkali treatment. Therefore, because the raw fiber contained the highest amorphous content, it was expected to have the lowest crystallinity index while the crystallinity index increased with retting time. The results showed that the crystallinity index dropped for the fiber retted for 8 h, which was attributable to fiber damage and the degradation of the cellulosic structure during the prolonged treatment of alkali. It has been reported that the crystallinity index equally depends on the pre-treatment method and the level of the fiber refining (Owolabi *et al.* 2017b). From the SEM image in Fig. 5e, the fiber subjected to a longer retting time (8 h) suffered damage through cell wall rupture, hence

accounting for the drop in the crystallinity index. This phenomenon also explained why the mechanical strength of the retted fiber at 8 h dropped compared with the 4-h retted *Typha* fiber.

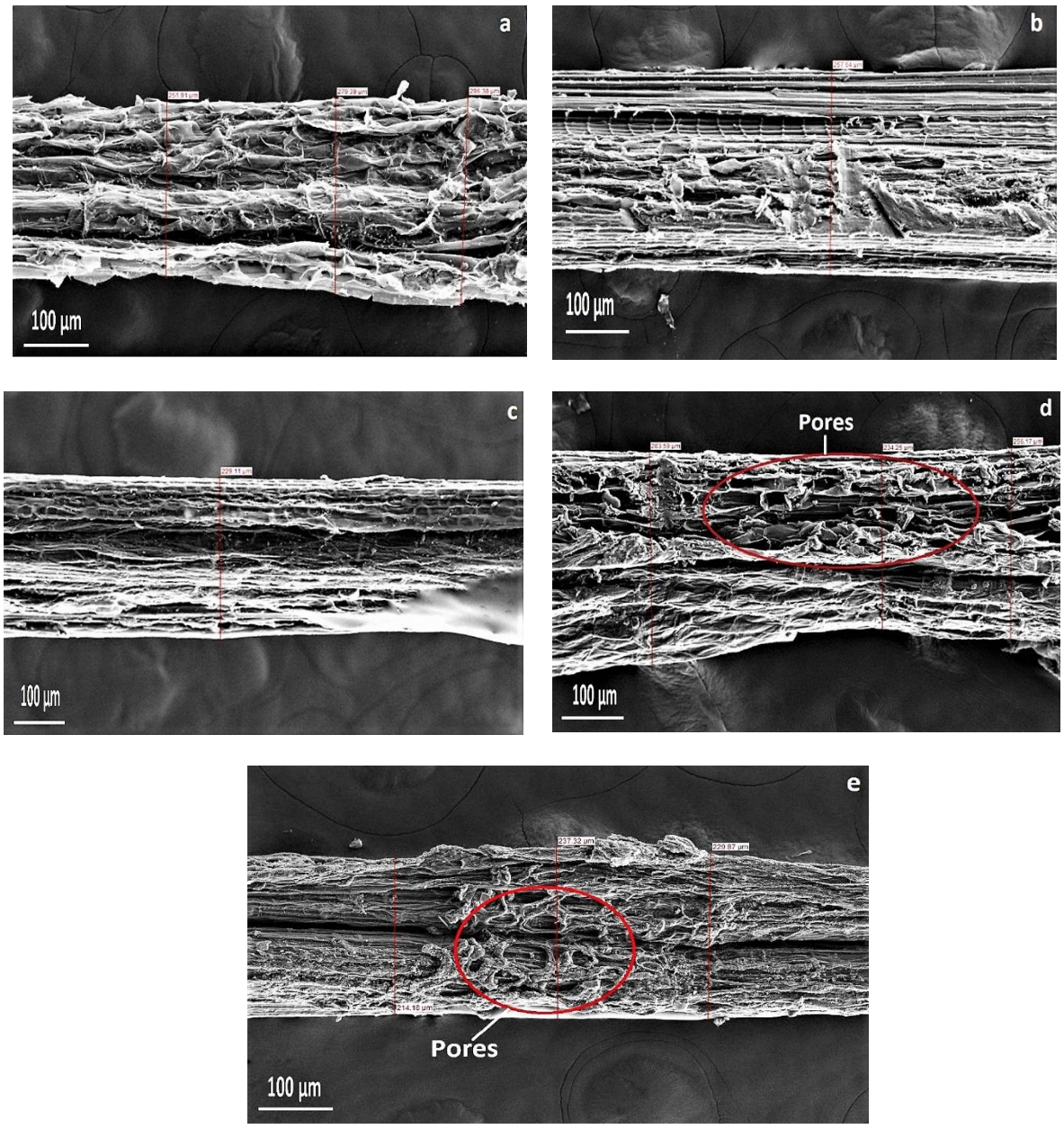

Fig. 5. Morphology of *Typha* fiber: (a) untreated; (b) alkali-treated for 1 h; (c) alkali-treated for 2 h; (d) alkali-treated for 4 h; and (e) alkali-treated for 8 h (magnification of 150×)

Morphology of the *Typha* Fiber

The *Typha* fiber morphology analysis was studied using SEM to evaluate the longitudinal surface structure of *Typha* fibers. The analysis of morphological changes in the fiber surface is important for understanding the roughness on the surface of *Typha* fibers due to the alkali treatment; it can further evaluate fiber interaction with the polymer matrix in the composite. Scanning electron micrographs of the untreated fibers are shown in Fig. 5a, and the fibers treated with alkali for 1 h, 2 h, 4 h, and 8 h are shown in Fig. 5b,

Fig. 5c, Fig. 5d, and Fig. 5e, respectively. The untreated *Typha* fibers were observed to contain many impurities on the fiber surface, but in the fibers treated with alkali for 1 h and 2 h, there were noticeable increases in the roughness of the *Typha* fiber surface and the fibers looked cleaner. Moreover, the fiber diameter also shrank after experiencing 1 h and 2 h of alkaline immersion, which occurred because some impurities, such as hemicellulose, lignin, pectin, and fatty substance, had been removed from the fiber surface. Therefore, the increase of the surface roughness resulted in increased adhesion between the fiber interface and the matrix in the composite (Ramesh *et al.* 2017). In Figs. 5d and 5e, it appears that the fibers soaked with NaOH for 4 h and 8 h made the fibers expand to larger diameters. The image at 8 h showed fiber damage as seen on the surface of the *Typha* fibers with the appearance of many pores, which was expected to affect the mechanism of wettability and bonding between the fiber and matrix. However, if the pores are more numerous, as in the alkali-treatment of 8 h, there will be a decrease in the mechanical properties of the fiber bundle (Hashim *et al.* 2017). This damage in *Typha* fiber was due to the prolonged treatment of *Typha* fiber with alkali.

Contact Angle Studies of *Typha* Fiber

Figure 6 shows the water contact angles of the untreated and alkali treated *Typha* fiber. In Fig. 6 it is clearly shown that the *Typha* fiber treated with alkali for 1 h showed the highest contact angle of water at an angle of 87.50°, while the untreated composite showed the lowest contact angle.

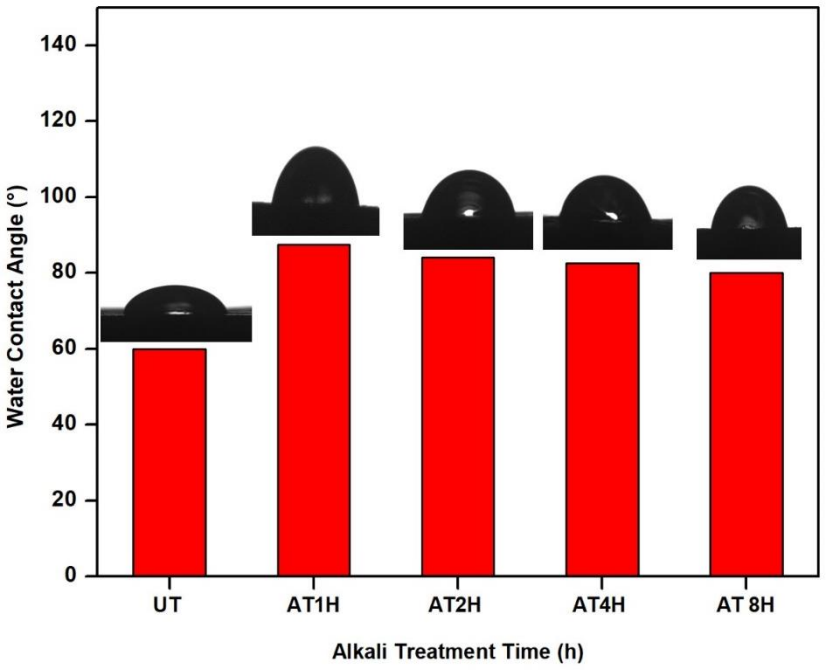

Fig. 6. Contact angle of the untreated and treated *Typha* fibers

The enhancement in the contact angle for the alkali-treated *Typha* fiber was attributed to the enhanced surface roughness of the fiber after alkali treatment (Chen *et al.* 2018). The hydrophilicity of the fibers was mainly influenced by two key factors: the surface roughness of the fiber and the availability or accessibility of hydroxyl groups in the fiber (Chowdhury *et al.* 2013). Throughout alkali treatment, the amorphous portions, such as hemicellulose, lignin, and wax, were removed from the *Typha* fiber, which led to the

reduction of the availability of hydroxyl groups in the fiber surface. Moreover, after alkali treatment, the surface of the *Typha* fiber became rougher, which resulted in the enhanced contact angle of the alkali treated *Typha* fiber when compared to the untreated ones. From the contact angle studies, it was concluded that after alkali treatment, the *Typha* fiber became hydrophobic in nature, which resulted in enhanced adhesion with the hydrophobic polymer matrices.

Mechanical Characterization

The mechanical characteristics of the *Typha* fiber examined included the tensile strength, Young's modulus, and elongation at break, as shown in Fig. 7a to Fig. 7c. Figures 7a through 7c show the average tensile strength, mean Young's modulus, and mean elongation at break of the *Typha* fiber at various retting times. From the results, it was shown that as the alkali treatment time increased, the mechanical properties increased with the retting time. The improvement in mechanical properties in the alkali-treated fiber was attributed to the removal of amorphous portions such as hemicellulose, lignin, pectin, and other waxy substances, from the *Typha* fiber surface during the alkali treatment, which resulted in the rougher topography.

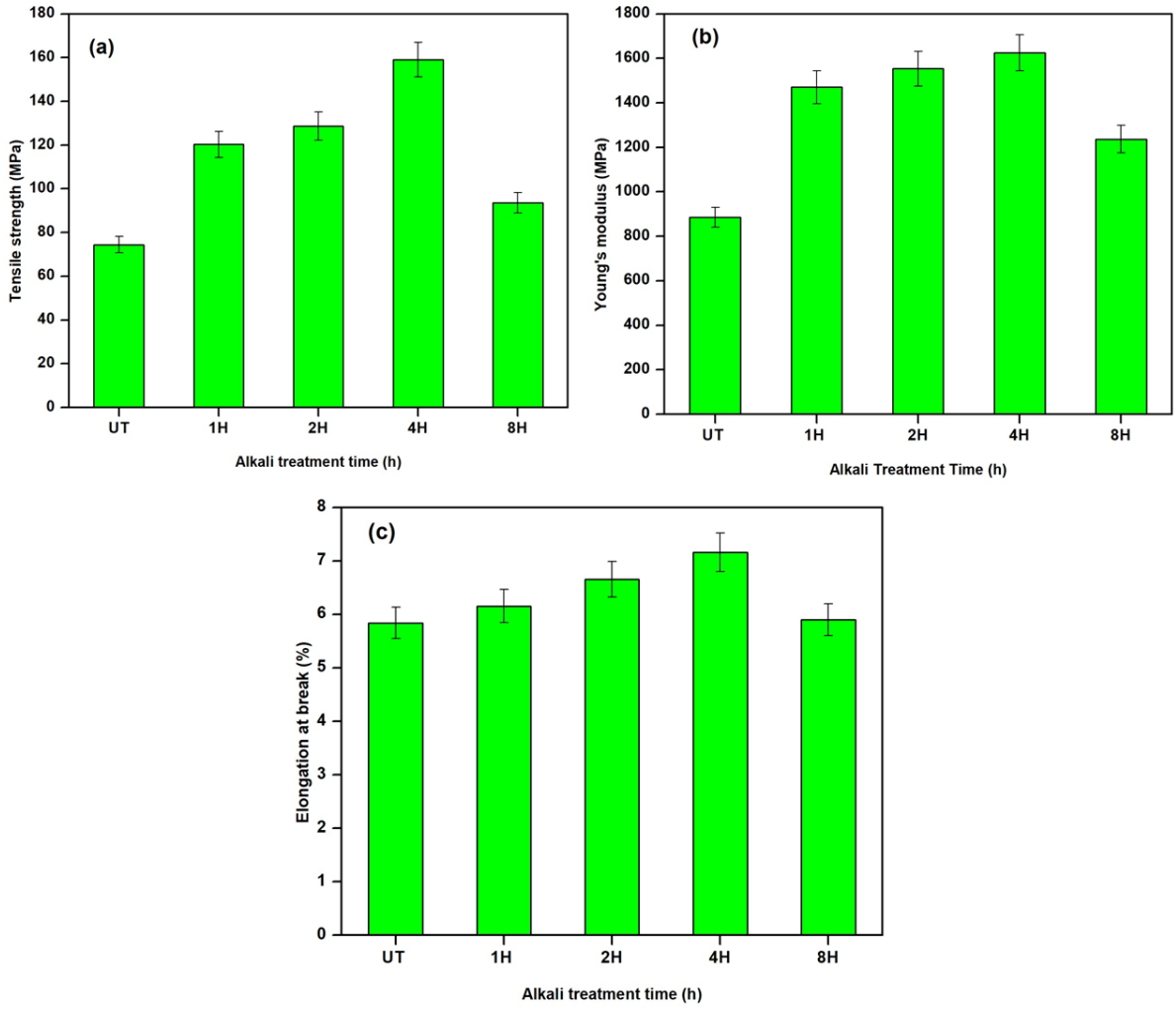

Fig. 7. Mechanical properties of *Typha* fiber: (a) tensile strength; (b) Young's modulus; and (c) elongation at break

As shown in Fig. 7, the mechanical properties of the *Typha* fibers were decreased after 4 h, and this was due to the degradation of the cellulosic structure of *Typha* fiber after the prolonged treatment with alkali. The removal of these amorphous portions promoted the intramolecular hydrogen bonding within the *Typha* leaf fiber. Conversely, the observed decrease in the mechanical strength at high alkali treatment was attributable to the damage to the fiber structure and the degradation of the cellulosic structure at higher alkali concentrations, as shown in the SEM images. This observation was comparable to the report of Mwaikambo and Ansell (1999), which stated that high alkaline concentrations would certainly damage the fiber and consequently reduce the mechanical strength of the fiber. A comparison of the effect of alkali treatment on the various type of natural fiber is presented in Table 1.

Table 1. Comparison of Mechanical Properties between *Typha* fiber and Other Alkali-treated Natural Fibers

Fiber Type	Alkali treatment percentage (exposure time)	Tensile strength (MPa)	Tensile modulus (GPa)	Elongation at break (%)	Reference
Ramie	15% (2 h)	151	-	-	(Goda *et al.* 2006)
Abaca fiber	5%, 10%, 15% (0.5 h)	847	24.3	4.5	(Cai *et al.* 2015)
Borassus fruit fine fibers	5% (1, 4, 8, 12 h)	121.3	35.2	58.1	(Obi Reddy *et al.* 2013)
Wheat straw fibers	15% (15 min)	146	7.9	-	(Panthapulakkal *et al.* 2006)
***Typha* fiber**	5% (1, 2, 4, 8h)	160	1.62	7.1	This study

Interfacial Shear Strength

The mechanical performances of a composite material strongly depend on the nature of the fibers, the nature of the matrix, and the quality of the interfacial shear strength (adhesion, IFSS) between the two components. Alkali-treated *Typha* fibers immersed for 8 h showed superior IFSS compared to the untreated fibers and fibers with alkali treatments of 1 h, 2 h, and 4 h. This indicated that the 8% alkali treated *Typha* fiber had good interfacial adhesion with both the epoxy and polyester, which resulted in a strong bonding mechanism. Figure 8a shows that the optimum average value of the IFSS for *Typha* fiber with epoxy was 4.7 MPa at 8 h, and this value was greater than the mean value of IFSS for *Typha* fiber with polyester of 3.7 MPa at 8 h, as shown in Fig. 8b. The IFSS values of the untreated *Typha* fibers were much lower than the IFSS values of the alkali treated *Typha* fiber, which increased with the duration of alkali treatment of the fiber. The low IFSS obtained for the untreated fiber was attributable to the presence of amorphous materials, such as hemicellulose, lignin, and pectin in the fibers, which interfered in the interfacial bonding between the materials. Untreated fibers are not compatible with hydrophobic polymers (epoxy and polyester resin) because the pectin and waxy substances in the untreated fiber act as a barrier to interlocking with the polymer matrix (Hashim *et al.* 2017). As the fiber extraction time increased, the amorphous portions, including hemicellulose, pectin, and other waxy substances, were removed from the fiber surface and resulted in the enhancement in the force of adhesion with excellent IFSS between the resins and the *Typha* fiber (Hao *et al.* 2018). In addition, the alkali treated *Typha* fiber surface was rougher than

the untreated fiber, which led to better mechanical interlocking. This mechanical interlocking mechanism can be optimized by increasing the surface roughness of the fibers and thus increasing the mechanical interlocking and adhesion between the fiber and matrix, both of which are responsible for the interfacial strength of the composite (Torstensen *et al.* 2018).

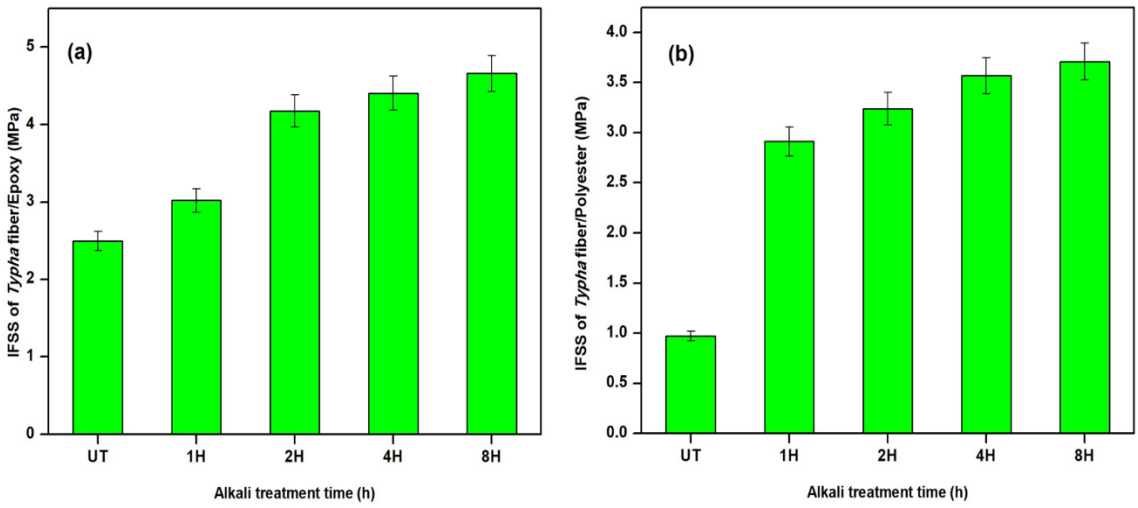

Fig. 8. (a) IFSS of *Typha* fiber/epoxy and (b) IFSS of *Typha* fiber/polyester

It was concluded that the mechanical interlocking phenomenon was dominant in the *Typha* fibers with alkali treatment durations of 4 h and 8 h, which was due to the penetration of resins into the holes, valves, and crevices on the surface of the *Typha* fibers. The pores in the alkali-treated surface of *Typha* fiber are clearly seen in Fig. 5d and Fig. 5e. Furthermore, the mechanical interlocking resulted in enhanced adhesion between the matrix and fibers, and therefore led to better bonding mechanisms. These results clearly showed that the alkali treatment for 8 h was the optimum concentration and duration to maximize the IFSS of the *Typha* fiber. With increasing adhesion between the fiber and matrix, the load applied to the fiber is still distributed to the matrix until the maximum force value is reached. After reaching the force value, the matrix will detach from the fiber, which is called debonding (Zukowski *et al.* 2018).

CONCLUSIONS

1. The alkali treatment of *Typha* fiber provided several effects, such as surface fiber modification, removal of fiber gluing materials from the fiber, and improvement of the mechanical properties of the polymer composite.
2. Alkali-treated *Typha* fiber had improved the mechanical and interfacial shear strength compared to the fiber without treatment. This was due to the removal of amorphous substances, such as hemicelluloses, lignin, and pectin, from the *Typha* fiber during the alkali treatment, as shown in the FTIR and XRD results.
3. It was concluded that the fiber surface became rougher after alkali treatment, which resulted in the better wettability with the hydrophobic polymer matrices.

4. *Typha* fibers with alkaline soaking for 4 h showed a higher crystallinity index, which resulted in better mechanical properties among the other treated fibers.
5. The highest IFSS was found in the 8 h of alkali-treated *Typha* fiber due to better mechanical interlocking behaviour, which resulted from the penetration of resins into the pores and the rougher surface of the alkali-treated *Typha* fiber.
6. Alkali-treated *Typha* fiber could be an effective candidate as a reinforcing agent in polymer composite material.

ACKNOWLEDGEMENTS

The authors wish to appreciate the collaborative efforts between the Department of Mechanical Engineering, Universitas Syiah Kuala, Indonesia and the School of Industrial Technology, Universiti Sains Malaysia for the successful completion of this research work. This work was supported by Ministry Research, Technology and Higher Education of Republic of Indonesia by World Class Professor (WCP), Program scheme No 123.5/D2.3/KP/2018 and Program Magister Menuju Doktor Untuk Sarjana Unggul (PMDSU).

REFERENCES CITED

Ahmad, F., Choi, H. S., and Park, M. K. (2015). "A review: Natural fiber composites selection in view of mechanical, light weight, and economic properties," *Macromolecular Materials and Engineering* 300(1), 10-24. DOI: 10.1002/mame.201400089

Al-Oqla, F. M., and Sapuan, S. M. (2014). "Natural fiber reinforced polymer composites in industrial applications: Feasibility of date palm fibers for sustainable automotive industry," *Journal of Cleaner Production*. 66, 347-354. DOI: 10.1016/j.jclepro.2013.10.050

Cai, M., Takagi, H., Nakagaito, A. N., Katoh, M., Ueki, T., Waterhouse, G. I. N., and Li, Y. (2015). "Influence of alkali treatment on internal microstructure and tensile properties of abaca fibers," *Industrial Crops and Products* 65, 27-35. DOI: 10.1016/j.indcrop.2014.11.048

Chen, H., Zhang, W., Wang, X., Wang, H., Wu, Y., Zhong, T., and Fei, B. (2018). "Effect of alkali treatment on wettability and thermal stability of individual bamboo fibers," *Journal of Wood Science*, Springer Japan, 64(4), 398-405. DOI: 10.1007/s10086-018-1713-0

Chowdhury, M. N. K., Beg, M. D. H., Khan, M. R., and Mina, M. F. (2013). "Modification of oil palm empty fruit bunch fibers by nanoparticle impregnation and alkali treatment," *Cellulose*, 20(3), 1477-1490. DOI: 10.1007/s10570-013-9921-7

Cohen, N., Dotan, A., Dodiuk, H., and Kenig, S. (2016). "Thermomechanical mechanisms of reducing ice adhesion on superhydrophobic surfaces," *Langmuir* 32(37), 9664-9675. DOI: 10.1021/acs.langmuir.6b02495

Fragassa, C., de Camargo, F. V., Pavlovic, A., and Minak, G. (2018). "Experimental evaluation of static and dynamic properties of low styrene emission vinylester laminates reinforced by natural fibres," *Polymer Testing* 69, 437-449. DOI:

10.1016/j.polymertesting.2018.05.050

Goda, K., Sreekala, M. S., Gomes, A., Kaji, T., and Ohgi, J. (2006). "Improvement of plant based natural fibers for toughening green composites—Effect of load application during mercerization of ramie fibers," *Composites Part A: Applied science and manufacturing* 37(12), 2213-2220. DOI: 10.1016/j.compositesa.2005.12.014

Hao, L. C., Sapuan, S. M., Hassan, M. R., and Sheltami, R. M. (2018). "Natural fiber reinforced vinyl polymer composites," in: *Natural Fibre Reinforced Vinyl Ester and Vinyl Polymer Composites*, S. M. Sapuan, H. Ismail, and E. S. Zainudin (eds.), Woodhead Publishing. DOI: 10.1016/B978-0-08-102160-6.00002-0

Hashim, M. Y., Amin, A. M., Marwah, O. M. F., Othman, M. H., Yunus, M. R. M., and Chuan Huat, N. (2017). "The effect of alkali treatment under various conditions on physical properties of kenaf fiber," in: *Journal of Physics: Conference Series*, Vol 914. DOI: 10.1088/1742-6596/914/1/012030

Ilyas, R. A., Sapuan, S. M., and Ishak, M. R. (2018a). "Isolation and characterization of nanocrystalline cellulose from sugar palm fibres (*Arenga pinnata*)," *Carbohydrate Polymers* 181, 1038–1051. DOI: 10.1016/j.carbpol.2017.11.045

Ilyas, R. A., Sapuan, S. M., Ishak, M. R., and Zainudin, E. S. (2017). "Effect of delignification on the physical, thermal, chemical, and structural properties of sugar palm fibre," *BioResources* 12(4), 8734–8754. DOI: 10.15376/biores.12.4.8734-8754

Ilyas, R. A., Sapuan, S. M., Ishak, M. R., and Zainudin, E. S. (2018b). "Development and characterization of sugar palm nanocrystalline cellulose reinforced sugar palm starch bionanocomposites," *Carbohydrate Polymers* 202, 186-202. DOI: 10.1016/j.carbpol.2018.09.002

Ilyas, R. A., Sapuan, S. M., Ishak, M. R., and Zainudin, E. S. (2018c). "Sugar palm nanocrystalline cellulose reinforced sugar palm starch composite: Degradation and water-barrier properties," in: *IOP Conference Series: Materials Science and Engineering*, IOP Publishing, 12006.

Jawaid, M., and Abdul Khalil, H. P. S. (2011). "Cellulosic/synthetic fibre reinforced polymer hybrid composites: A review," *Carbohydrate Polymers* 86(1), 1-18. DOI: 10.1016/j.carbpol.2011.04.043

Karger-Kocsis, J., Mahmood, H., and Pegoretti, A. (2015). "Recent advances in fiber/matrix interphase engineering for polymer composites," *Progress in Materials Science* 73, 1-43. DOI: 10.1016/j.pmatsci.2015.02.003

Khalil, H. P. S. A., Ismail, H., Rozman, H. D., and Ahmad, M. N. (2001). "Effect of acetylation on interfacial shear strength between plant fibres and various matrices," *European Polymer Journal* 37(5), 1037-1045. DOI:10.1016/S0014-3057(00)00199-3

Loh, Y. R., Sujan, D., Rahman, M. E., and Das, C. A. (2013). "Review. Sugarcane bagasse - The future composite material: A literature review," *Resources, Conservation and Recycling* 75, 14-22. DOI: 10.1016/j.resconrec.2013.03.002

Łojewska, J., Miśkowiec, P., Łojewski, T., and Proniewicz, L. M. (2005). "Cellulose oxidative and hydrolytic degradation: In situ FTIR approach," *Polymer Degradation and Stability*. 88(3), 512-520. DOI: 10.1016/j.polymdegradstab.2004.12.012

Majeed, K., Jawaid, M., Hassan, A., Abu Bakar, A., Abdul Khalil, H. P. S., Salema, A. A., and Inuwa, I. (2013). "Potential materials for food packaging from nanoclay/natural fibres filled hybrid composites," *Materials and Design* 46, 391-410. DOI: 10.1016/j.matdes.2012.10.044

Miller, B., Muri, P., and Rebenfeld, L. (1987). "A Microbond Method for Determination

of the Shear Strength of a Fiber/ Resin Interface," *Composites Science and Technology*, 28(1), 17-32. DOI: 10.1016/0266-3538(87)90059-5

Mwaikambo, L. Y., and Ansell, M. P. (1999). "The effect of chemical treatment on the properties of hemp, sisal, jute and kapok for composite reinforcement," *Die Angewandte Makromolekulare Chemie* 272(1), 108-116. DOI: 10.1002/(SICI)1522-9505(19991201)272:1<108::AID-APMC108>3.0.CO;2-9

Nacos, M. K., Katapodis, P., Pappas, C., Daferera, D., Tarantilis, P. A., Christakopoulos, P., and Polissiou, M. (2006). "Kenaf xylan - A source of biologically active acidic oligosaccharides," *Carbohydrate Polymers* 66(1), 126-134. DOI: 10.1016/j.carbpol.2006.02.032

Obi Reddy, K., Uma Maheswari, C., Shukla, M., Song, J. I., and Varada Rajulu, A. (2013). "Tensile and structural characterization of alkali treated Borassus fruit fine fibers," *Composites Part B: Engineering* 44(1), 433-438. DOI: 10.1016/j.compositesb.2012.04.075

Owolabi, A. F., Haafiz, M. K. M., Hossain, M. S., Hussin, M. H., and Fazita, M. R. N. (2017a). "Influence of alkaline hydrogen peroxide pre-hydrolysis on the isolation of microcrystalline cellulose from oil palm fronds," *International Journal of Biological Macromolecules* 95, 1228-1234. DOI: 10.1016/j.ijbiomac.2016.11.016

Owolabi, A. F., Saurabh, C. K., Dungani, R., and Abdul Khalil, H. P. S. (2017b). "Spectroscopy and microscopy of microfibrillar and nanofibrillar composites," in: *Micro and Nano Fibrillar Composites (MFCs and NFCs) from Polymer Blends*, S. Thomas, R. Mishra, and N. Kalarikkal (eds.), Woodhead Publishing, DOI: 10.1016/B978-0-08-101991-7.00012-1

Panthapulakkal, S., Zereshkian, A., and Sain, M. (2006). "Preparation and characterization of wheat straw fibers for reinforcing application in injection molded thermoplastic composites," *Bioresource Technology* 97(2), 265-272. DOI: 10.1016/j.biortech.2005.02.043

Ramesh, M., Palanikumar, K., and Reddy, K. H. (2017). "Plant fibre based bio-composites: Sustainable and renewable green materials," *Renewable and Sustainable Energy Reviews* 79, 558-584. DOI: 10.1016/j.rser.2017.05.094

Ramezani Kakroodi, A., Kazemi, Y., and Rodrigue, D. (2013). "Mechanical, rheological, morphological and water absorption properties of maleated polyethylene/hemp composites: Effect of ground tire rubber addition," *Composites Part B: Engineering* 51, 337-344. DOI: 10.1016/j.compositesb.2013.03.032

Sanjay, M. R., Arpitha, G. R., Naik, L. L., Gopalakrishna, K., and Yogesha, B. (2016). "Applications of natural fibers and its composites: An overview," *Natural Resources*. 7(3), 108-114. DOI: 10.4236/nr.2016.73011

Sanjay, M. R., Madhu, P., Jawaid, M., Senthamaraikannan, P., Senthil, S., and Pradeep, S. (2018). "Characterization and properties of natural fiber polymer composites: A comprehensive review," *Journal of Cleaner Production* 172, 566-581. DOI: 10.1016/j.jclepro.2017.10.101

Sanyang, M. L., Ilyas, R. A., Sapuan, S. M., and Jumaidin, R. (2018). "Sugar palm starch-based composites for packaging applications," in: *Bionanocomposites for Packaging Applications*, Springer, pp. 125-147.

Sassoni, E., Manzi, S., Motori, A., Montecchi, M., and Canti, M. (2014). "Novel sustainable hemp-based composites for application in the building industry: Physical, thermal and mechanical characterization," *Energy and Buildings* 77, 219-226. DOI: 10.1016/j.enbuild.2014.03.033

Shalwan, A., and Yousif, B. F. (2013). "In state of art: Mechanical and tribological behaviour of polymeric composites based on natural fibres," *Materials and Design* 48, 14-24. DOI: 10.1016/j.matdes.2012.07.014

da Silva, L. F. M., Öchsner, A., and Adams, R. D. (2018). "Introduction to adhesive bonding technology," *Handbook of Adhesion Technology*, Second Edition, Springer. DOI: 10.1007/978-3-319-55411-2_1

Sun, C., Wang, Y., Wang, Z., Chen, H., Wang, X., Li, H., Sun, L., Fan, C., Wang, C., and Zhang, X. (2018). "Fabrication of hierarchical ZnSAPO-34 by alkali treatment with improved catalytic performance in the methanol-to-olefin reaction," *Comptes Rendus Chimie*. 21(1), 61-70. DOI: 10.1016/j.crci.2017.11.006

Taylor, C., Amiri, A., Paramarta, A., Ulven, C., and Webster, D. (2017). "Development and weatherability of bio-based composites of structural quality using flax fiber and epoxidized sucrose soyate," *Materials and Design* 113, 17-26. DOI: 10.1016/j.matdes.2016.10.002

Torstensen, J. Ø., Liu, M., Jin, S.-A., Deng, L., Hawari, A. I., Syverud, K., Spontak, R. J., and Gregersen, Ø. W. (2018). "Swelling and free-volume characteristics of TEMPO-oxidized cellulose nanofibril films," *Biomacromolecules* 19(3), 1016-1025. DOI: 10.1021/acs.biomac.7b01814

Le Troedec, M., Sedan, D., Peyratout, C., Bonnet, J. P., Smith, A., Guinebretiere, R., Gloaguen, V., and Krausz, P. (2008). "Influence of various chemical treatments on the composition and structure of hemp fibres," *Composites Part A: Applied Science and Manufacturing* 39(3), 514-522. DOI: 10.1016/j.compositesa.2007.12.001

Xiong, X., Shen, S. Z., Hua, L., Liu, J. Z., Li, X., Wan, X., and Miao, M. (2018). "Finite element models of natural fibers and their composites: A review," *Journal of Reinforced Plastics and Composites* 37(9), 617-635. DOI: 10.1177/0731684418755552

Zhao, S., Teng, J., Wang, Z., Sun, X., and Yang, B. (2018). "Investigation on the mechanical properties of SMA/GF/Epoxy hybrid composite laminates: Flexural, impact, and interfacial shear performance," *Materials* 11(2), article E236. DOI: 10.3390/ma11020246

Zukowski, B., de Andrade Silva, F., and Toledo Filho, R. D. (2018). "Design of strain hardening cement-based composites with alkali treated natural curauá fiber," *Cement and Concrete Composites* 89, 150-159. DOI: 10.1016/j.cemconcomp.2018.03.006

Article submitted: Jan. 8, 2019; Peer review completed: May 12, 2019; Revised version received and accepted: May 23, 2019; Published: May 31, 2019.
DOI: 10.15376/biores.14.3.5630-5645